BMC Cancer

RESEARCH

Open Access

Reductive prodrug and AIE copolymer nanoparticle for monitoring and chemotherapy

Zigui Wang[1,2,3,4], Guilin Li[4], Qiaohui Zhao[4], Guangyu Fu[5], Zengli Yang[5] and Guojun Zhang[1,2,3*]

Abstract

Polymeric micelle systems for drug delivery, monitor and chemotherapy have gained significant attention, and reductive polymeric micelle systems have become particularly attractive due to their controlled release behavior without additional assistance. However, there are challenges in accurately controlling drug and probe release from the nanoparticles and determining the loading content of drug and probe. To address these issues, we have developed a reduction-responsive Pt(IV) prodrug-based polymeric delivery system that can be dynamically monitored using aggregation-induced emission luminogens (AIE) based bioprobes. These polymeric micelle can self-assemble into nanoparticles and release both bio-active Pt(II) drug and bio-probe upon reduction activation. TPE molecules released in the inner endo/lysosomal microenvironment aggregate and fluoresce upon irradiation, thus allowing real-time tracking of drug biodistribution without additional contrast agents. Advantages of this system include position-specific chemical bond cleavage, control of platinum content, and monitoring of drug reduction and biodistribution.

Keywords AIE, Chemotherapy, Platinum, Drug delivery, Real-time tracing

Introduction

Recently, there has been a surge in interest in advanced polymeric micelle delivery systems for controlled and targeting chemotherapy and simultaneous drug tracking [1, 2]. Various stimuli, such as pH, redox, oxidative stress, temperature, and light, have been utilized to control drug release in these systems [3–7]. Among these, reductive polymeric micelle systems have attracted great attention due to their low toxicity and ability to achieve controlled release without ex vivo stimuli or assistance. Current design for formation of prodrug nanoparticles are mainly about drugs encapsulated into nanoparticles with stimuli molecules on the key chemical bond of polymer or conjugation of the drug to the polymer through a linker to form prodrug nanoparticles are among the most common strategies [8, 9]. However, these traditional polymeric micelles may exhibit variable drug release behaviors, posing challenges for precise release control within the body (in vivo). Additionally, the loading content of drugs remains uncertain with common encapsulation methods, which complicated drug release in body or targeted cancer regions [10]. Furthermore, real-time monitoring of drug distribution in the body is currently not feasible. The use of fluorescent agents or other contrast agents for diagnostic imaging in therapeutics increases the complexity and cost of synthesis or manufacturing and can lead to unforeseen adverse side effects [11–13]. These challenges significantly limit the widespread application of polymeric micelle systems and new design or synthetic strategies are highly needed for more precisely control and real-time monitoring [14].

*Correspondence:
Guojun Zhang
guojun.zhang@ccmu.edu.cn
[1] Department of Clinical Diagnosis, Laboratory of Beijing Tiantan Hospital, Capital Medical University, Beijing, China
[2] NMPA Key Laboratory for Quality Control of In Vitro Diagnostics, Beijing, China
[3] Beijing Engineering Research Center of Immunological Reagents Clinical Research, Beijing, China
[4] Zhengzhou Immunobiotech Co, Ltd, Zhengzhou 450016, P.R. China
[5] Autobio Diagnostics Co, LtdHenan 450016, China

Another challenge in real-time tracking and therapy systems is the inability to precisely monitor the time it takes for drug concentrations to accumulate at tumor sites and other organs, such as the heart, liver, spleen, lung, and kidney [15, 16]. With this regard, we hypothesize that integrating fluorescent molecules into reduction-responsive polymeric delivery systems could enable dynamic monitoring of drug biodistribution. Among all the current imaging diagnostic techniques, there are mainly fluorescence imaging, positron emission tomography (PET)/CT and magnetic resonance imaging (MRI) [17–20]. Due to CT's high resolution and deep tissue penetration, it is the most commonly used diagnostic technique in clinical practice. However, used small molecular CT contrast agents like iohexol and iodixanol were difficult to conjugated it to polymer. Besides, these have drawbacks such as rapid blood clearance, high viscosity, and high osmolality, which limited its application [21, 22]. Some fluorescence molecules can be utilized to construct fluorescent nanoprobe with low toxicity and minimal side effects but traditional dyes often suffer from aggregation-caused quenching (ACQ) when assembled into aggregate [23–26]. On the contrary, bioprobes based on aggregation-induced emission (AIE) exhibit attractive features in monitoring cell molecules with huge potential [22]. Recently, AIE has been polymerized into polymer backbone to develop AIE polymeric nanoparticles for drug delivery [7]. Nevertheless, the fluorescence of AIE polymeric nanoparticles is consistently active everywhere without specificity due to the intramolecular motion mechanism of AIE. To achieve in situ activation of AIE polymeric nanoparticles at target sites, intricate molecular design and modification are required for the system.

Recently, we have synthesised a series of reductive Pt(IV) prodrug-based polymeric delivery systems for low side chemotherapy [2, 27]. However, dynamically monitoring the spatiotemporal distribution of drugs at tumor sites and other organs remains challenging. As a cytotoxic platinum(II) (Pt(II)) prodrug, a hydrophobic platinum(IV) (Pt(IV)) complex has many advantages, such as higher stability and lower cytotoxicity, which could undergo reduction to bio-active Pt(II) inside cancer cells [28–31]. Thus, a Pt(IV) complex can be conjugated to polymeric key joint and be released in a controlled fashion at tumor site, serving as both a drug and reduction-responsive moiety [32]. To combine the advantages of aggregation-induced emission luminogens based bioprobes and Pt(IV) complexes, we constructed polymeric micelles by conjugating hydrophobic Pt(IV) inside the polymeric chain and the monitor molecules TPE conjugated on the Pt(IV) molecules, which can self-assemble into nanoparticles (PAGE-Pt-TPE) in water solution. After cancer cells swallow PAG-PT-TPE, the chemical bond between the polymer and Pt(IV) will be broken by reduction of GHS, and the Pt(IV) prodrug in the core of PAG-PT-TPE will be activated to release the active Pt(II) drug, including DNA damage. Subsequently, TPE released under the acidic endo/lysosome microenvironment would aggregate and fluoresce upon irradiation, thereby enabling real-time tracing (Scheme 1). The PAGE-Pt-TPE system possesses several advantages: (1) Activation of tumor site-specific chemical bond cleavage by reducing agents triggers release of Pt(II) drugs and biological probes without the introduction of additional ACQ. (2) Prodrug Pt(IV) conjugated in polymer chain side enable precise control the content of Pt. (3) PAGE-Pt-TPE is expected to be able to monitor the cleavage of polymeric micelle. The reduction of prodrug Pt(IV) to active Pt(II) was monitored to dynamically monitor the biodistribution of the drug without additional contrast agents. Additionally, the fluorescence intensity can also reflect the sensitivity of tumor cells to drugs.

Experiment

Materials and Measurements

Cisplatin was bought from Shandong Boyuan Chemical Company, China.1-(4-Aminophenyl)-1,2,2-triphenylethene, N-hydroxysuccinimide (NHS), pyridine, 1-ethyl-3-(3-dimethylaminopropyl) carbodiimide hydrochloride (EDC), methoxy polyethylene glycol (Mn = 8000 Da,

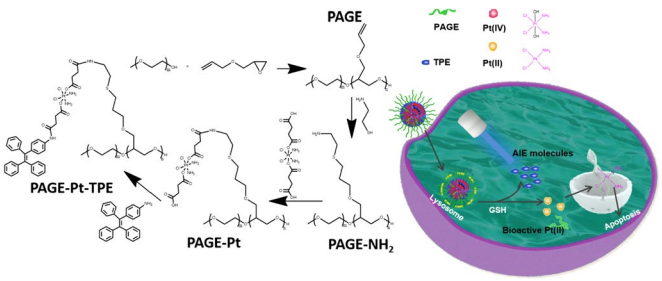

Scheme 1 Schematic diagram of reductive prodrug and AIE copolymer micelles for monitoring and chemotherapy

$mPEG_{8k}$), 3-(4,5-dimethylthiazol-2-yl)-2,5-diphenyltetrazolium bromide (MTT), Allyl glycidyl ether (AGE), 2,2'-Azobis(2-methylpropionitrile) (AIBN), succinic anhydride 1-(4-Aminophenyl)-1,2,2-triphenylethene (TPE) and 2-Aminoethanethiol hydrochloride were purchased from Aladdin Chemistry Co. Ltd. (Shanghai, China). All other reagents were commercially available and used as received.

Measurements

Proton nuclear magnetic resonance (^{1}HNMR) spectra were measured on a Bruker AVANCE DRX 400 spectrometer using deuterated dimethyl sulfoxide (DMSO d_6) and deuterium oxide (D_2O). The molecular weight and polydispersity index of the synthetic polymer were detected using a Tetrahydrofuran 515 gel permeation chromatograph (GPC). Diameter and polydispersity index were measured on Malvern ZETASIZER LAB. Transmission electron microscope (TEM) images were collected using a JEOL JEM-1011 transmission electron microscope with an acceleration voltage of 100 kV. An inductively coupled plasma mass spectrometer (ICP-MS, Xseries II, Thermo Fisher Scientific, USA) was used for the analysis content of Pt. Electrospray ionization mass spectrometry (ESI–MS) measurement was conducted on a Waters Quattro Premier XE system. The molecular weight and polydispersity index of the synthetic polymer were determined using a Tetrahydrofuran 515 gel permeation chromatograph (GPC). The molecular weight of PAGE-Pt-TPE was analyzed by using Autof ms800 (Autobio Diagnostics, Zhengzhou, China) systems.

Synthesis of Pt(IV) prodrug

Briefly, cisplatin (1 g) was suspended in H_2O_2 (20 mL, 30%) stirred for 24 h at room temperature. Finally, Pt(IV) was obtained by filtration and washing with water and ethanol.

Synthesis of Pt(IV)-COOH

The Pt(IV) prodrug (1 g, 2.9 mmol) and succinic anhydride (1.168 g, 11.6 mmol) were dissolved in N,N-Dimethylformamide (DMF, 20 ml). After reaction at 60 ℃ for 24 h, solution was poured into diethyl ether and filtering it for three time.

Synthesis of PAGE

Block copolymer PAGE was synthesized according to the literature with a slight change as shown in Scheme 1. Briefly, dried $mPEG_{8k}$(2.0 mmol), 305 mg cesium hydroxide monohydrate (1.8 mmol, 0.9 equiv), and 40 mL dried toluene were added to a dry reaction bulb under argon/nitrogen atmosphere. In order to acquire partially deprotonated macroinitiator, it is necessary to evacuate at 90 ℃ for 3 h. After that, additional 100 mL of toluene was added and 6.84 g AGE (60.0 mmol, 15 equiv) was added. The polymerization reaction needs to be maintained for 48 h at 45 ℃ for 48 h under an inert atmosphere. To stop the polymerization was stopped, a trace of acetic acid–ethanol (50/50) solution was added.The reaction solution was poured into a mount of cold diethyl ether for 3 times and the polymers were collected and dried in vacuum for 8 h (85%).

Synthesis of PAGE-NH_2

PAGE (5 g), 2-Aminoethanethiol hydrochloride (10 g, 62.5 mmol) and dried 20 mL of DMF were add to dry reaction bulb under inert atmosphere. After dissolution and addition of AIBN, the reaction maintained for 24 h at 65 ℃ under an inert atmosphere. DMF was removed at 50 ℃ under vacuum. Residue was redissovled in CH_2Cl_2 and precipitated in cold diethyl ether. After filtered and dried, mPEG-NH_2 was acquired.

Synthesis of PAGE-Pt

In general, large excess of Pt(IV)-COOH prodrug (245 mg, 0.46 mmol), EDC (265 mg, 1.38 mmol), and NHS (159 mg, 1.38 mmol) were added into reaction bulb and 8 mL of DMF was injected. The solution was activated for 4 h in ice bath. After that, poured PEGA-NH_2 (184 mg, 0.023 mmol) into reaction solution and maintained the reaction at 25 ℃ for 3 days. Finally, the solution was poured into Spectra/Por Regenerated Cellulose membrane (MWCO = 3500), which was dialyzed with purified water for 2 days. After freeze-dried, PAGE-Pt was obtained.

Synthesis of PAGE-Pt-TPE

In general, PAGE-Pt polymeric prodrug (100 mg, 0.01 mmol), EDC (46 mg, 0.24 mmol), and NHS (28 mg, 0.24 mmol) were added into reaction bulb and 8 mL of DMF was injected. The solution was activated for 4 h in ice bath. After that, poured TPE (69.4 mg, 0.2 mmol) into reaction solution and maintained the reaction at 25 ℃ for 3 days. Finally, the solution was poured into Spectra/Por Regenerated Cellulose membrane (MWCO = 3500), which was dialyzed with purified water for 2 days. After freeze-dried, PAGE-Pt-TPE was obtained.

Reductive drug release of PGAE-Pt-TPE

To simulate the release process of PAGE-Pt-TPE in vivo. PAGE-Pt-TPE (2 mg) was dissolved in different phosphate buffer, inluding 1 mL of PBS (0.01 M, pH 7.4), PBS (0.01 M, pH 7.4, 1 mg/ml SA), PBS (0.01 M, pH 5.0) or PBS (0.01 M, pH 5.0, 1 mg/ml SA). The solution was poured into a dialysis bag (MWCO = 500) and 19 mL of

the corresponding PBS solutions was added. Drug release was conducted at 37 ℃ in an air bath shaker.

Cell culture

Human cervical carcinoma HeLa cells were cultured with Dulbecco's modified Eagle's medium containing 10% fetal bovine serum (FBS). The U14 cells were cultured in the ascites of mice. These and murine tumor cells U14 were acquired from the Institute of Biochemistry and Cell Biology, Chinese Academy of Sciences, Shanghai, China.

Cellular uptake of TPE

For TPE release in cells, The germfree coverslips were added into 6-well plates. HeLa cells were cultured on it (2×10^{5} cells per well) for 24 h. PAGE-Pt-TPE was dissolved in DMEM (Pt: 54 μM) and the initial medium was substituted with PAGE-Pt-TPE solution for 2 h and 4 h, respectively. After cultured for corresponding time, HeLa cells were washed with cold PBS. For CLSM observation, the HeLa cells on the coverslips were fixed using formaldehyde(4%) for 15 min 25 ℃. We observed fluorescence images using a CLSM.

Cell viability

Cells were seeded in 96-well plates (5×10^{3} cells per well). After incubated in DMEM for 24 h, the medium was added with cisplatin, TPE, Pt(IV), PAGE-Pt and PAGE-Pt-TPE from 3.375 to 216 μM (final Pt concentration from or equal molar amount Pt). After incubating for 48 h, MTT was added, and 96-well plates was at incubator for another 4 h. Afer removal of MTT solution, 150 mL of DMSO was added to each well to dissolve the formazan crystals formed in the cells. After mixed for 5 min, the absorbance was acquired at 490 nm using a microplate reader.

Animals used

Kunming (KM) mice were bought from Jilin University. The experimental mice bearing U14 xenograft tumor model were acquired by subcutaneously injecting U14 cells (1×10^{6}, 0.1 mL PBS) into right legs of mice. All the in vivo study protocols were approved by the local institution review board and performed according to the Ethics Committee of the Beijing Tiantan Hospital of Capital Medical University, China. After volume of subcutaneous U14 tumor model reach to 500 mm^3, the animals were anaesthetized with pentobarbital sodium and the tumor was collected from sacrificed mice. It was cut into pieces and treated with homogenizer and pressure cell disruptor. After that, supernatant was collected by centrifugation.

Results and discussion

Pt(II) drugs have been extensively utilized in the treatment of various cancers over the past decades, yet their application has been hindered by severe side effects. Pt(IV) prodrugs, particularly those with reductive properties, have shown promise as a preferable option to mitigate toxic side effects. In this study, a reductive Pt(IV) prodrug was integrated with TPE as a fluorescence molecule, initially coupled with the Pt(IV) prodrug to produce amphiphilic PAGE-Pt-TPE.obtain amphiphilic PAGE-Pt-TPE. The successful synthesis of PAGE, PAGE-NH_2, PAGE-Pt was confirmed by ^{1}H NMR and GPC was also conducted to characterize the molecular weight of PAGE-Pt (Mn = 14,500 Da, PDI = 1.13 Fig. S3). The peak at δ = 3.51 ppm could be assigned to $-NH_3$ of Pt(IV) in DMSO d_6, which indicates the successful synthesis of Pt(IV) (Fig. 1A). As can be seen in Fig. 1B, PAGE displayed the ^{1}H NMR signals of mPEG (3.65 ppm), AGE (c at ~ 5.3 ppm, d at ~ 5.9 ppm, and b at ~ 4.0 ppm). After reaction with 2-aminoethanethiol hydrochloride, the ^{1}H NMR all the signals of AGE (c at ~ 5.3 ppm, d at ~ 5.9 ppm, and b at ~ 4.0 ppm) disappeared in DMSO d_6 (Fig. 1C, which indicates that PAGE-NH_2 was prepared. To synthesis PAGE-Pt, PEGA-NH_2 and Pt(IV) were stirred at room temperature for 3 days. As shown in Fig. 1D, PAGE-Pt displayed the ^{1}H NMR signals of Pt(IV) (-NH_3, 6.5 ppm).

Block copolymer PAGE-Pt-TPE could self-assemble into nanoparticles in aqueous solution, as demonstrated (characterized) TEM with a diameter was about 150 nm (Fig. 2A). The diameter was about 150 nm. Furthermore, the morphology and size changes of PAGE-Pt-TPE nanoparticles after reduction were monitored using TEM and DLS, respectively. PAGE-Pt-TPE nanoparticles exhibited uniform and regular spherical morphology before treated with SA (5×10^{-3} M), while as shown in Fig. 2B, it became highly polydisperse in shape and size after treated with SA (5×10^{-3} M). Following reduction, the hydrophilic and hydrophobic balance of PAGE-Pt-TPE nanoparticles shifted, leading to a loosening of the nanoparticle structure due to reductive dissociation. Furthermore, the contrast became shallower, consistent with the DLS results (Fig. 2C and D). The values of polydispersity index(PDI) for PAGE-Pt-TPE nanoparticles was 0.69, but after treated with SA, the PDI was 0.82, which was ascribed to disassemble of micelles.

In order to further prove the successful synthesis of the PAGE-Pt-TPE, it was also confirmed by ^{1}H NMR in different solvent. The peak at δ = 7.0 ppm and 8.0 ppm as shown in Fig. 3A, could be assigned to ^{1}H of benzene ring in DMSO d_6. As shown in Fig. S4, the molecular weight of PAGE-Pt-TPE was about 23,411, which indicted that the molecule TPE was conjugated to PAGE-Pt successfully.

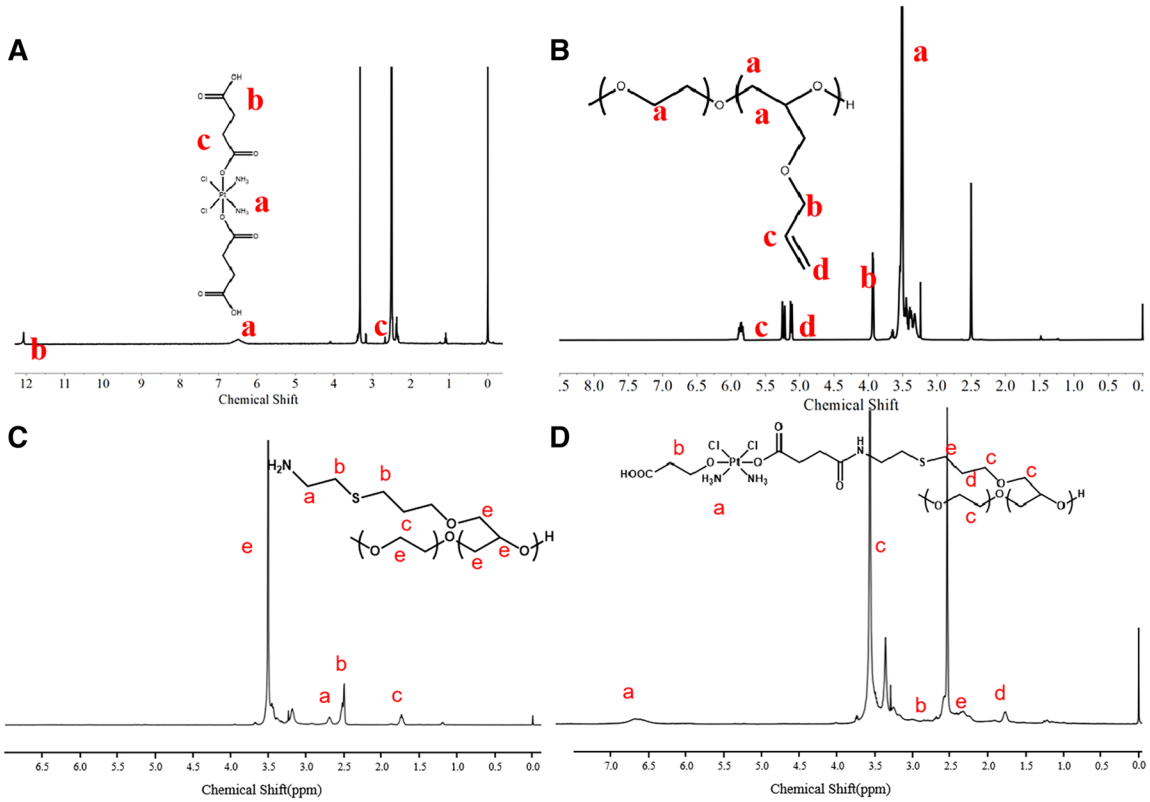

Fig. 1 The characteristics of Pt(IV), PAGE, PAGE-NH_2 and PAGE-Pt**.** ^{1}H NMR spectrum of **A** Pt(IV), **B** PAGE, **C** PAGE-NH2 and **D** PAGE-Pt in DMSO

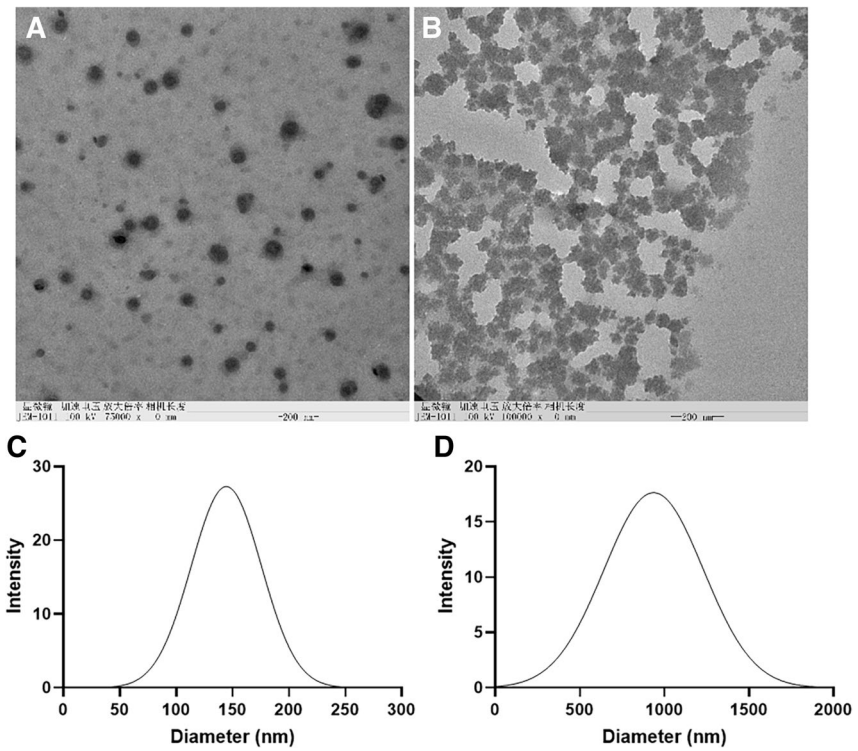

Fig. 2 Characterization of reduction-sensitive self-assembled PAGE-Pt-TPE. TEM images of PAGE-Pt-TPE) before and **B** after treated with SA (5×10^{-3} M) for 24 h. Size distribution of PAGE-Pt-TPE **C** before and **D** after treated with SA (5×10^{-3} M) for 24 h

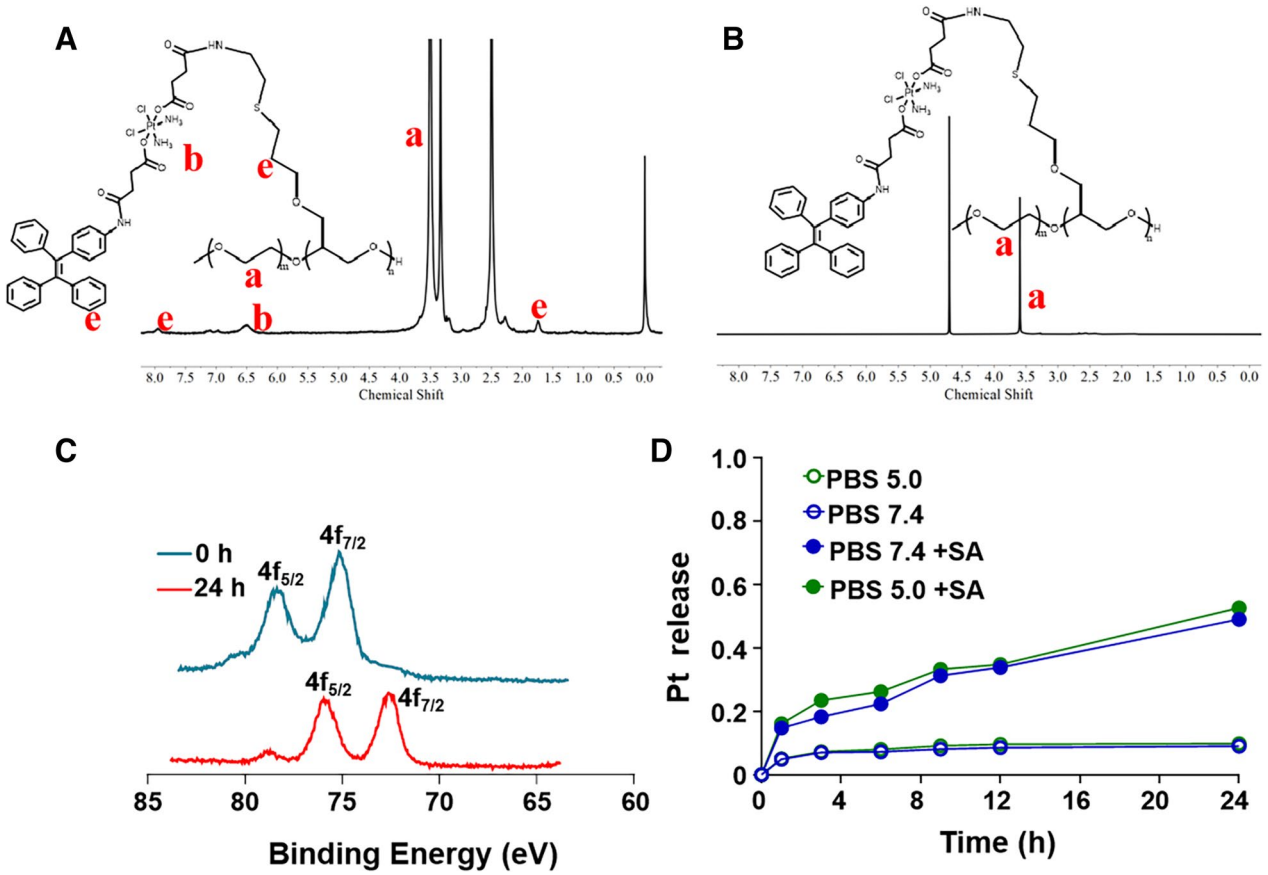

Fig. 3 Characterization of PAGE-Pt-TPE and Pt release profiles of PAGE-Pt-TPE. ^{1}H NMR spectrum of PAGE-Pt-TPE in **A** DMSO and **B** in D_2O. **C** XPS curves of Pt_{4f} in PAGE-Pt-TPE micelles before and after treated with SA for 0 h and 24 h; **D** Pt release profiles of PAGE-Pt-TPE in different media (PBS 5.0, PBS 7.4, PBS7.4 with SA and PBS 5.0 with SA)

As previously mentioned, block copolymer PAGE-Pt-TPE could self-assemble into nanoparticles in aqueous solution, which was important for drug delivery system and imaging system. The effective tumor accumulation of nanoparticles/micelles caused by the enhanced permeability and retention (EPR) effect made it possible for passive targeted killing of tumor cells. The successful synthesis of PAGE-Pt-TPE was also proved by ^{1}H NMR. As shown in Fig. 3B, Compared with the ^{1}H NMR spectrum in DMSO d_6, all of the peaks of PAGE-Pt-TPE except the peak of the $mPEG_{5k}$ (-OCH_2CH2-, $\delta = 3.51$ ppm) disappeared in D_2O, which indicates that PAGE-Pt-TPE self-assembled into micelles in aqueous solution. XPS was also conducted to characterize the change in Pt valence in PAGE-Pt-TPE before and after reduction. As displayed in Fig. 3C, Pt_{4f} in the PAGE-Pt-TPE before reduction exhibited the characteristic binding energies of Pt(IV) (78.5 and 75.2 eV). After reduction, the Pt_{4f} binding energies in the low-molecular-weight species were 75.8 eV and 72.6 eV, which indicates the reduction of Pt(IV) prodrug and the release of the bioactive Pt(II). The release of the bioactive Pt(II) implied fragmentation of the micelles. The reductive Pt release profiles from PAGE-Pt-TPE were further investigated. Though our previous literature research, the intracellular pH value is low. PBS 5.0 solution was used to simulate the release process of PAGE-Pt-TPE in vivo. SA was used to simulate the cell's reductive environment.[5] As shown in Fig. 3D, the release percentage of Pt was only 10% after 24 h without reducing agent, while treated with SA for 1 h, approximately 16% of Pt was released from PAGE-Pt-TPE After treated with SA for 24 h, 52% of Pt was released from PAGE-Pt-TPE. These results indicated that PAGE-Pt-TPE was very susceptible to reduction, and the drug release could be precisely controlled by endocytosis.

As we know, AIE is a phenomenon that is observed with certain organic luminophores (fluorescent dyes).[7] Due to ACQ, The photoemission efficiencies of most organic compounds is higher in solution or dispersity than in the solid state. But some organic molecules follows the reverse pattern, being greater in the solid than in dispersity or solution. The effect is attributed to the

decreased kinetic energy in the solid. To demonstrate the advantages of combination of TPE and Pt(IV), the luminescence phenomenon of PAGE-Pt-TPE aqueous solutions was detected treated with different concentration SA and the fluorescence spectra of PAGE-Pt-TPE solutions at different concentration. As shown in Fig. 4A, PAGE-Pt-TPE expressed fluorescence intensity, but the fluorescence intensity become stronger when the concentration increase from 1 mg/ml to 2 mg/ml. After treated with SA, PAGE-Pt-TPE expressed intense fluorescence at the same concentration. These results indicate that micelles PAGE-Pt-TPE could improve the solubility of TPE leading to weaker fluorescence, but after treated with reduction, TPE released from PAGE-Pt-TPE and generated agglomeration.

The cytotoxicity tests of PAGE-Pt-TPE against HeLa cells cells were conducted by using cisplatin, Pt(IV), PAGE-Pt, TPE as controls. As shown in Figs. 4B and C, after treatment for 48 h, the IC_{50} value of PAGE-Pt and PAGE-Pt-TPE (10.7 μM) showed much higher cytotoxicity than that of the cisplatin (17.2 μM) and Pt(IV) (158 μM). All the results confirm the cytotoxicity of PAGE-Pt-TPE in vitro. To visualize the internalization process and Imaging effect, the fluorescence monitoring of PAGE-Pt-TPE in cancer cells was investigated by CLSM. After incubation with HeLa cells for 0 h, none blue fluorescence from TPE was observed in cytoplasm (Fig. 4D). But after incubation for 2 and 4 h, strong blue fluorescence was observed in cytoplasm. TPE reflects the process of drug release and the fluorescence intensity can also reflect the sensitivity of tumor cells to drugs.

After volume of subcutaneous U14 tumor model reach to 500 mm^3, the tumor was collected from sacrificed mice. The supernatant was treated with PAGE-Pt-TPE for 12 h at 37 ℃ in a shaking culture incubator. As shown in Fig. 4E, both supernatant without any treatment and treated with PAGE-Pt-TPE nanoparticles for 0 h had no fluorescence under light irradiation at 365 nm. But 12 h later, the sample treated with PAGE-Pt-TPE emitted strong fluorescence, while the other sample did not. Therefore, PAGE-Pt-TPE micelles can release TPE at tumor microenvironment. At the same time, drug release and distribution were tracked.

Conclusion

In summary, we have developed a PAGE-Pt-TPE micelle system for precise chemotherapy guided by AIE imaging without ACQ. The PAGE-Pt-TPE system enables the reduction-triggered release of the Pt(IV) prodrug, resulting in the release of bioactive Pt(II) drug within cancer cells or at the

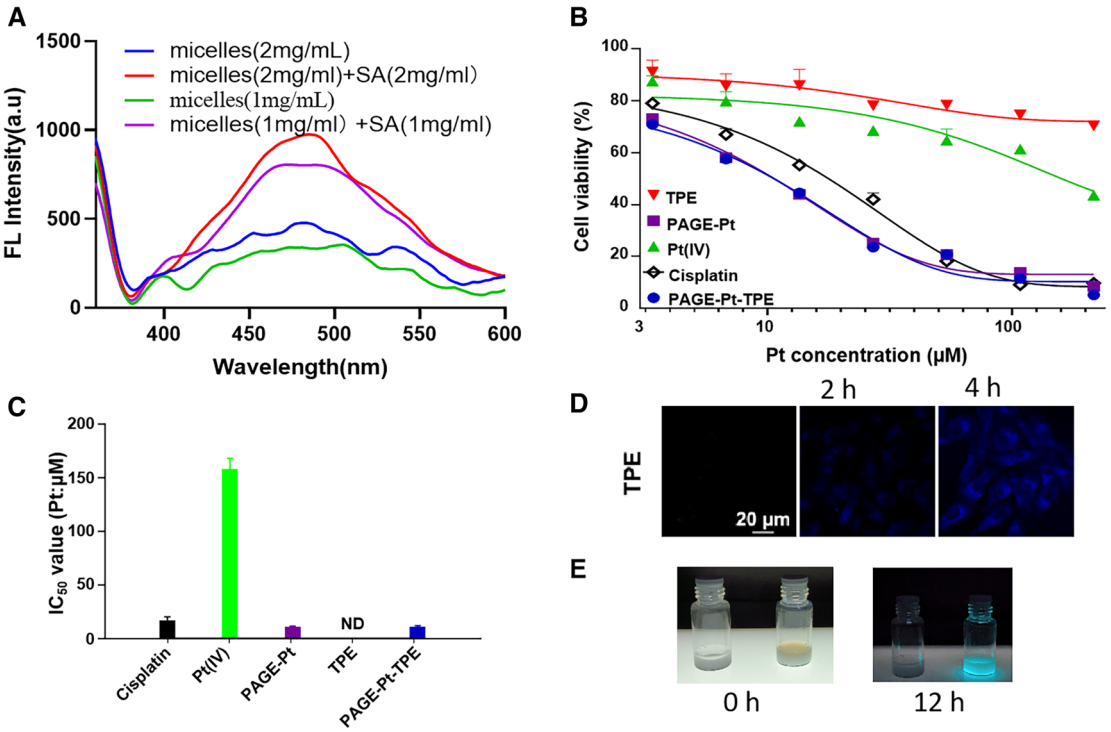

Fig. 4 In vitro cytotoxicity profiles and action mechanism of PAGE-Pt-TPE**. A** Fluorescence spectra of PAGE-Pt-TPE before and after treated with different concentration SA; **B** cytotoxicity curves against HeLa cells after 48 h of incubation **C** IC_{50} of different samples **D** CLSM images of HeLa cells pre-treating with PAGE-Pt-TPE incubation for 2 h and 4 h in the dark at 37 ℃. **E** The change of tumor's supernatant pre-treating with PAGE-Pt-TPE for 12 h

tumor site. Additionally, the cleaved polymer segment further reduces to produce TPE, leading to AIE both in vitro and in vivo. Moreover, these micelles hold potential for diagnostic applications. For instance, if modified with targeted molecules or specific antibodies, they can accumulate at specific sites and emit a fluorescent signal. It will spread rang of application if broaden the wavelength range of TPE.

Author' contributions

ZGW wrote the main manuscript text; GLL, QHZ, GYF and ZLY prepared all the figures. All authors reviewed the manuscript .

Supplementary Information

The online version contains supplementary material available at https://doi.org/10.1186/s12885-024-12135-7.

Supplementary Material 1.

Acknowledgements
Not applicable.

Author contributions
ZGW wrote the main manuscript text; GLL, QHZ, GYF and ZLY prepared all the figures. All authors reviewed the manuscript.

Funding
This study was supported by Beijing Municipal Natural Science Foundation (code: NO.7222052), Beijing Hospitals Authority Clinical Medicine Development of Special Funding Support (code: ZYLX202108), Beijing Hospitals Authority's Ascent Plan (DFL20220505) and Beijing High-level Public health technical Personnel Training program (2022–2-013).

Data Availability
The datasets used and/or analysed during the current study available from the corresponding author Guojun Zhang (guojun.zhang@ccmu.edu.cn) on reasonable request.

Declarations

Ethics approval and consent to participate
Our study was conducted in accordance with the Declaration of Helsinki and the study protocol was approved by the Ethics Committee of the Beijing Tiantan Hospital of Capital Medical University, China (KY 2020–076-02). All the related animals are euthanized. The study was carried out in compliance with the ARRIVE guidelines.

Consent for publication
Not applicable.

Competing interests
The authors declare no competing interests.

Received: 1 December 2023 Accepted: 17 March 2024
Published online: 26 March 2024

References

1. Ghosh B, Biswas S. Polymeric micelles in cancer therapy: State of the art. J Control Release. 2021;332:127–47.
2. Wang Z, Wu P, He Z, He H, Rong W, Li J, Zhou D, Huang Y. Mesoporous silica nanoparticles with lactose-mediated targeting effect to deliver platinum(iv) prodrug for liver cancer therapy. J Mater Chem B. 2017;5(36):7591–7.
3. Xiao H, Noble GT, Stefanick JF, Qi R, Kiziltepe T, Jing X, Bilgicer B. Photosensitive Pt(IV)–azide prodrug-loaded nanoparticles exhibit controlled drug release and enhanced efficacy in vivo. J Controlled Release. 2014;173:11–7.
4. He S, Qi Y, Kuang G, Zhou D, Li J, Xie Z, Chen X, Jing X, Huang Y. Single-Stimulus Dual-Drug Sensitive Nanoplatform for Enhanced Photoactivated Therapy. Biomacromol. 2016;17(6):2120–7.
5. Gao J, Meng Q, Zhao Y, et al. EHD1 confers resistance to cisplatin in non-small cell lung cancer by regulating intracellular cisplatin concentrations. BMC Cancer. 2016;16:470.
6. Wang Z, Kuang G, Yu Z, Li A, Zhou D, Huang Y. Light-activatable dual prodrug polymer nanoparticle for precise synergistic chemotherapy guided by drug-mediated computed tomography imaging. Acta Biomater. 2019;94:459–68.
7. Wu P, Wang X, Wang Z, Ma W, Guo J, Chen J, Yu Z, Li J, Zhou D. Light-Activatable Prodrug and AIEgen Copolymer Nanoparticle for Dual-Drug Monitoring and Combination Therapy. ACS Appl Mater Interfaces. 2019;11(20):18691–700.
8. Saito G, Swanson JA, Lee KD. Drug delivery strategy utilizing conjugation via reversible disulfide linkages: role and site of cellular reducing activities. Adv Drug Res. 2003;55(2):199–215.
9. Spiers L, Gray M, Lyon P, et al. Clinical trial protocol for PanDox: a phase I study of targeted chemotherapy delivery to non-resectable primary pancreatic tumours using thermosensitive liposomal doxorubicin (ThermoDox®) and focused ultrasound. BMC Cancer. 2023;23:896.
10. Stenzel MH. The Trojan Horse Goes Wild: The Effect of Drug Loading on the Behavior of Nanoparticles. Angew Chem Int Ed Engl. 2021;60(5):2202–6.
11. Chertok B, Moffat BA, David AE, Yu F, Bergemann C, Ross BD, Yang VC. Iron oxide nanoparticles as a drug delivery vehicle for MRI monitored magnetic targeting of brain tumors. Biomaterials. 2008;29(4):487–96.
12. van der Meel R, Sulheim E, Shi Y, Kiessling F, Mulder WJM, Lammers T. Smart cancer nanomedicine. Nat Nanotechnol. 2019;14(11):1007–17.
13. Yan GP, Robinson L, Hogg P. Magnetic resonance imaging contrast agents: Overview and perspectives. Radiography. 2007;13:e5–19.
14. Ghezzi M, Pescina S, Padula C, Santi P, Del Favero E, Cantù L, Nicoli S. Polymeric micelles in drug delivery: An insight of the techniques for their characterization and assessment in biorelevant conditions. J Controlled Release. 2021;332:312–36.
15. Baetke SC, Lammers T, Kiessling F. Applications of nanoparticles for diagnosis and therapy of cancer. Br J Radiol. 2015;88(1054):20150207.
16. Wang X, Li S, Wang S, Zheng S, Chen Z, Song H. Protein Binding Nanoparticles as an Integrated Platform for Cancer Diagnosis and Treatment. Adv Sci. 2022;9(29):2202453.
17. Mariani G, Bruselli L, Kuwert T, Kim EE, Flotats A, Israel O, Dondi M, Watanabe N. A review on the clinical uses of SPECT/CT. Eur J Nucl Med Mol Imaging. 2010;37(10):1959–85.
18. Katti G, Ara SA, Shireen A. Magnetic resonance imaging (MRI)–A review. Int J Dent Clin. 2011;3(1):65–70.
19 Rao J, Dragulescu-Andrasi A, Yao H. Fluorescence imaging in vivo: recent advances. Curr Opin Biotechnol. 2007;18(1):17–25.
20. Wang S, Ren WX, Hou J-T, Won M, An J, Chen X, Shu J, Kim JS. Fluorescence imaging of pathophysiological microenvironments. Chem Soc Rev. 2021;50(16):8887–902.
21. Yin Q, Yap FY, Yin L, Ma L, Zhou Q, Dobrucki LW, Fan TM, Gaba RC, Cheng J. Poly(iohexol) Nanoparticles As Contrast Agents for in Vivo X-ray Computed Tomography Imaging. J Am Chem Soc. 2013;135(37):13620–3.
22. Ding D, Li K, Liu B, Tang BZ. Bioprobes Based on AIE Fluorogens. Acc Chem Res. 2013;46(11):2441–53.
23. Mérian J, Gravier J, Navarro F, Texier I. Fluorescent Nanoprobes Dedicated to in Vivo Imaging: From Preclinical Validations to Clinical Translation. Molecules. 2012;17(5):5564–91.
24. Chen M, Yin M. Design and development of fluorescent nanostructures for bioimaging. Prog Polym Sci. 2014;39(2):365–95.
25. Qi J, Hu X, Dong X, Lu Y, Lu H, Zhao W, Wu W. Towards more accurate bioimaging of drug nanocarriers: turning aggregation-caused quenching into a useful tool. Adv Drug Deliv Rev. 2019;143:206–25.
26. Yuan WZ, Lu P, Chen S, Lam JWY, Wang Z, Liu Y, Kwok HS, Ma Y, Tang BZ. Changing the Behavior of Chromophores from Aggregation-Caused

Quenching to Aggregation-Induced Emission: Development of Highly Efficient Light Emitters in the Solid State. Adv Mater. 2010;22(19):2159–63.
27. He S, Li C, Zhang Q, Ding J, Liang X-J, Chen X, Xiao H, Chen X, Zhou D, Huang Y. Tailoring Platinum(IV) Amphiphiles for Self-Targeting All-in-One Assemblies as Precise Multimodal Theranostic Nanomedicine. ACS Nano. 2018;12(7):7272–81.
28. Johnstone TC, Suntharalingam K, Lippard SJ. The Next Generation of Platinum Drugs: Targeted Pt(II) Agents, Nanoparticle Delivery, and Pt(IV) Prodrugs. Chem Rev. 2016;116(5):3436–86.
29. Ravera M, Gabano E, McGlinchey MJ, Osella D. A view on multi-action Pt(IV) antitumor prodrugs. Inorg Chim Acta. 2019;492:32–47.
30. Rottenberg S, Disler C, Perego P. The rediscovery of platinum-based cancer therapy. Nat Rev Cancer. 2021;21(1):37–50.
31. Ghosh S. Cisplatin: The first metal based anticancer drug. Bioorg Chem. 2019;88: 102925.
32. Miller MA, Zheng Y-R, Gadde S, Pfirschke C, Zope H, Engblom C, Kohler RH, Iwamoto Y, Yang KS, Askevold B, Kolishetti N, Pittet M, Lippard SJ, Farokhzad OC, Weissleder R. Tumour-associated macrophages act as a slow-release reservoir of nano-therapeutic Pt(IV) pro-drug. Nat Commun. 2015;6(1):8692.

Publisher's Note